A Biomass Experimental Data

Table S1: wood biomass data for generation of model. HR = heating rate. Estimated values marked with orange.

Biomass	**Equip.**	**Size** mm	**final T** K	**HR** K/s	**K content** wt % daf	**Char yield** wt % daf	**Reference**
Pinewood	DTF	0.3125	1273	5747	0.02	3.2	S1
Beechwood	DTF	0.3125	1273	4382	0.37	7.8	S1
Pinewood	DTF	0.3125	1523	9336	0.02	2.8	S1
Beechwood	DTF	0.3125	1523	7093	0.37	6.6	S1
Pinewood	DTF	0.3125	1673	12208	0.02	2.8	S1
Beechwood	DTF	0.3125	1673	9259	0.37	6.3	S1
Pinewood	WMR	0.125	873	1000	0.02	7.5	S2
Beechwood	WMR	0.125	873	1000	0.36	12.6	S2
Pinewood	WMR	0.125	1273	1000	0.02	5.9	S2
Beechwood	WMR	0.125	1273	1000	0.36	10.6	S2
Beechwood	WMR	0.125	1523	1000	0.36	8.4	S2
Pinewood	WMR	0.125	1273	100	0.02	8.3	S2
Beechwood	WMR	0.125	1273	100	0.36	15.1	S2
Pinewood	WMR	0.125	1273	300	0.02	7.2	S2
Beechwood	WMR	0.125	1273	300	0.36	13.5	S2
Pinewood	WMR	0.125	1273	600	0.02	7.0	S2
Beechwood	WMR	0.125	1273	600	0.36	11.8	S2
Pinewood	WMR	0.125	1273	3000	0.02	5.7	S2
Beechwood	WMR	0.125	1273	3000	0.36	8.9	S2
Pinewood	WMR	0.125	873	1000	0.02	5.1	S2
Pinewood	WMR	0.3025	873	1000	0.02	5.9	S2
Pinewood	WMR	0.39	873	1000	0.02	7.6	S2
Pinewood	WMR	0.5125	873	1000	0.02	7.2	S2
Pinewood	WMR	0.725	873	1000	0.02	7.6	S2
Pinewood	WMR	0.925	873	1000	0.02	7.6	S2
Pinewood	WMR	0.125	1273	1000	0.02	5.8	S2
Pinewood	WMR	0.3025	1273	1000	0.02	5.9	S2
Pinewood	WMR	0.39	1273	1000	0.02	6.0	S2
Pinewood	WMR	0.5125	1273	1000	0.02	6.2	S2
Pinewood	WMR	0.725	1273	1000	0.02	7.0	S2
Pinewood	WMR	0.925	1273	1000	0.02	7.2	S2
Pinewood	WMR	0.125	1523	1000	0.02	4.2	S2
Pinewood	WMR	0.3025	1523	1000	0.02	4.4	S2
Pinewood	WMR	0.39	1523	1000	0.02	4.6	S2
Pinewood	WMR	0.5125	1523	1000	0.02	4.7	S2
Pinewood	WMR	0.725	1523	1000	0.02	4.8	S2
Pinewood	WMR	0.925	1523	1000	0.02	7.2	S2

Table S2: Biomass data for evaluation of model. Estimated values marked with orange. Woody biomass above dashed line. Herbaceous biomass below dashed line.

Biomass	Equip.	Size [mm]	final Temp. K	HR K/s	K content wt % daf	Char Yield wt % (daf)	Reference
Pinewood	EFR	0.3025	1273	6040	0.0332	2.4	S3
Beechwood sawdust	EFR	0.3025	1273	4604	0.0955	6.1	S3
Pinewood	EFR	0.3025	1573	10721	0.0332	2.0	S3
Beechwood sawdust	EFR	0.3025	1573	8138	0.0955	4.7	S3
Beech for food smoking	DTF	0.3565	1273	3601	0.090	3.9	S4
Beech for food smoking	DTF	0.815	1273	1183	0.082	5.2	S4
Beech for food smoking	DTF	0.3565	1473	5349	0.090	3.8	S4
Beech for food smoking	DTF	0.815	1473	1811	0.082	3.3	S4
Beech for food smoking	DTF	0.3565	1673	7704	0.090	2.4	S4
Beech for food smoking	DTF	0.815	1673	2689	0.082	3.3	S4
Hinoki cypress sawdust	DTR	0.25	1273	11997	0.03	4.0	S5
beech wood	DTR	0.35	1073	2393	0.05	5.4	S6
Cynara Cardunculus thistle	EFR	0.35	1073	10000	>0.53	15.3	S7
Cynara Cardunculus thistle	EFR	0.35	1203	10000	>0.53	11.8	S7
Cynara Cardunculus thistle	EFR	0.35	1313	10000	>0.53	14.3	S7
Cynara Cardunculus thistle	EFR	0.35	1448	10000	>0.53	15.3	S7

B Estimating the Missing Parameters

Table S4: The experimentally specific variables necessary for estimating the Heating Rate.

Symbol	Description	Unit
D_p	Diameter of particle	m
T_{end}	Final Temperature of particle	K

Table S5: The parameters to be calculated for estimating the Heating Rate.

Symbol	Description	Unit
$C_{p,g}$	Specific heat capacity of gas	$J/(kg \cdot K)$
k	Thermal conductivity	$J/(s \cdot m \cdot K)$
T	Half way Temperature in particle	K
v_{slip}	slip velocity	m/s
μ	Dynamic Viscosity	$Pa \cdot s$
ρ_g	Density of carrier gas	kg/m^3

Table S3: wood biomass data for evaluation of model. Estimated values marked with orange.

Biomass	**Equip.**	**Size** [mm]	**final Temp.** K	**HR** K/s	**K content** wt % daf	**Char Yield** wt % (daf)	**Reference**
Straw	DTF	0.3125	1273	10000	1.1	7.14	S1
Straw	DTF	0.3125	1523	10000	1.1	5.29	S1
Straw	DTF	0.3125	1673	10000	1.1	2.96	S1
Straw	WMR	0.125	873	1000	1.1	21.7	S2
Straw	WMR	0.125	1273	1000	1.1	14.26	S2
Straw	WMR	0.125	1523	1000	1.1	11.49	S2
Straw	WMR	0.125	1673	1000	1.1	10.21	S2
Straw	WMR	0.125	1273	100	1.1	18.51	S2
Straw	WMR	0.125	1273	300	1.1	16.41	S2
Straw	WMR	0.125	1273	600	1.1	15.37	S2
Straw	WMR	0.125	1273	3000	1.1	12.12	S2
Straw	WMR	0.125	873	1000	1.1	15.83	S2
Straw	WMR	0.3025	873	1000	1.1	16.25	S2
Straw	WMR	0.39	873	1000	1.1	17.5	S2
Straw	WMR	0.5125	873	1000	1.1	15.83	S2
Straw	WMR	0.725	873	1000	1.1	15	S2
Straw	WMR	0.925	873	1000	1.1	15	S2
Straw	WMR	0.125	1273	1000	1.1	13.56	S2
Straw	WMR	0.3025	1273	1000	1.1	13.56	S2
Straw	WMR	0.39	1273	1000	1.1	13.73	S2
Straw	WMR	0.5125	1273	1000	1.1	14.41	S2
Straw	WMR	0.725	1273	1000	1.1	14.07	S2
Straw	WMR	0.925	1273	1000	1.1	14.24	S2
Straw	WMR	0.125	1523	1000	1.1	10.71	S2
Straw	WMR	0.3025	1523	1000	1.1	10.26	S2
Straw	WMR	0.39	1523	1000	1.1	11.28	S2
Straw	WMR	0.5125	1523	1000	1.1	12.18	S2
Straw	WMR	0.725	1523	1000	1.1	12.18	S2
Straw	WMR	0.925	1523	1000	1.1	12.52	S2

Table S6: The constants necessary for estimating the heating rate. Values assumed from literature.

Symbol	Description	Value	Unit	Reference
$C_{p,p}$	Specific heat capacity of particle	$1500 + T_i$	$J/(kg \cdot K)$	[S8]
g	gravity acceleration constant	9.81	m/s^2	
R	Gas constant	$8.206 \cdot 10^{-5}$	$m^3 \cdot atm\ /(K \cdot mol)$	
ρ_{hinoki}	Density hinoki cypress	400	kg/m^3	[S9]
ρ_{pine}	Density pine wood	600	kg/m^3	[S10]
ρ_{beech}	Density beech	800	kg/m^3	[S10]
σ	Stefan-Boltzmann constant	$5.670367 \cdot 10^{-8}$	$J/(s \cdot m^2 \cdot K^4)$	[S11]
ϵ	Emissivity Coefficient	0.85	-	[S12]

B.1 Assumptions

The estimate of the heating rate is based on a number of assumptions given in the list below.

A The heating rate can be represented by a single value even though it varies with time and location in the particle.

B Particles are spherical

C Particle size can be approximated with average of the sieve sizes.

D Particles are uniform, i.e. no pores.

E Particles are isothermal.

F Particle properties as for example density are uniform throughout the particle.

G No chemical reaction adds to the energy balance.

H All gasses are inert and ideal.

I The temperature around the particle can be approximated as the average between the initial and the final temperatures.

J Initial gas temperature is 298 K.

B.2 Temperature Dependent Properties of Nitrogen

From NIST [S13] the properties are collected as temperature dependent properties if nothing else is noted. The carrier gas is nitrogen for all relevant biomass data given in table S1 and S2. Correlation and calculations analogue to the ones presented below can be found for other gasses if relevant. The properties of the carrier gas are temperature dependent. Here the temperature for the estimation is defined in equation (1).

$$T = T_{ini} + \frac{T_{end} - T_{ini}}{2} \tag{1}$$

B.2.1 Density of Nitrogen

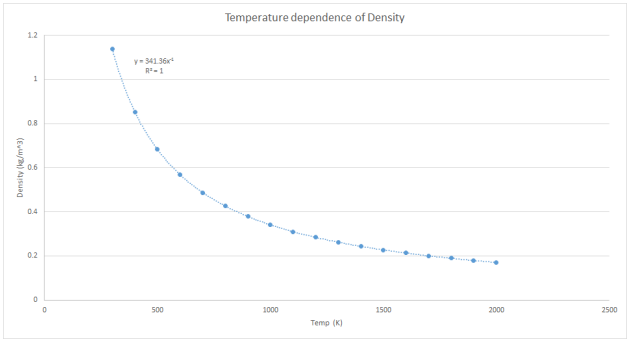

Figure S1: The correlation between Density and Temperature for N_2. Data from NIST.[S13]

The density temperature correlation is given in equation (2).

$$\rho_{N_2} = 341.36 \frac{1}{T_g} \tag{2}$$

B.2.2 Heat capacity of Nitrogen

$$C_p = A + B \cdot \frac{T_g}{1000} + C \cdot \left(\frac{T_g}{1000}\right)^2 + D \cdot \left(\frac{T_g}{1000}\right)^3 + E \cdot \left(\frac{1000}{T_g}\right)^2 \tag{3}$$

Where the constants are given in table S7.

Table S7: Constants for the Shomate Equation for Nitrogen in the interval 500-2000 K.

A	B	C	D	E
19.50583	19.88705	-8.598535	1.369784	0.527601

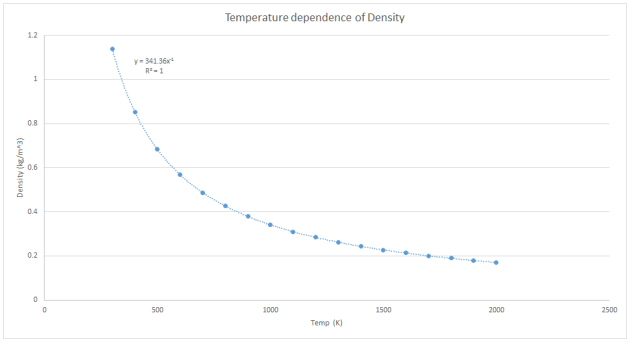

Figure S2: The correlation between Heat Capacity and Temperature for N_2. Data from NIST.[S13]

B.2.3 Viscosity of Nitrogen

Data from NIST. A third degree polynomial is fitted to the data, which yields $R^2 = 1$. Gives the correlation given in equation (4). As this polynomial is fitted to the given data it is only valid in the temperature range 300-2000 K.

$$\mu_g = 3 \cdot 10^{-9} \cdot T_g^3 - 2 \cdot 10^{-5} \cdot T_g^2 + 0.0508 \cdot T_g + 4.2787 \tag{4}$$

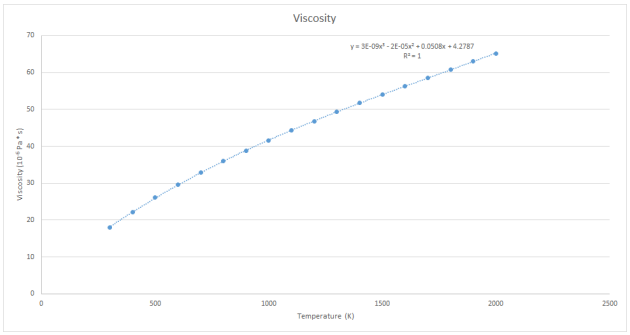

Figure S3: The correlation between Viscosity and Temperature for N_2. Data from NIST.[S13]

B.2.4 Thermal Conductivity of Nitrogen

Data from NIST. A second degree polynomial is fitted to the data, which yields $reg^2 = 1$. Gives the correlation given in equation (4). As this polynomial is fitted to the given data it is only valid in the temperature range 300-2000 K.

$$k = -7 \cdot 10^{-9} \cdot T_g^2 + 7 \cdot 10^{-5} \cdot T_g + 0.0069 \tag{5}$$

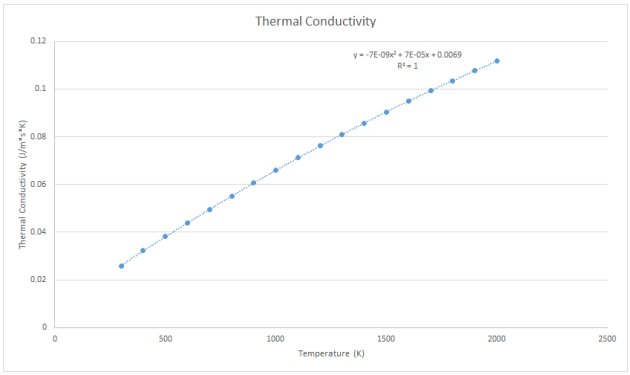

Figure S4: The correlation between Conductivity and Temperature for N_2. Data from NIST.[S13]

B.3 Calculating the Reynolds Number and Prandtl Number

The Reynolds Number for a sphere in a fluid is given by equation (6).[S14]

$$Re_p = \frac{\rho_g \cdot v_p \cdot D_p}{\mu} \tag{6}$$

Where ρ_g is the density of the carrier gas (here N_2), v_p is the particle velocity as calculated in equation (7) or (8),[S15*]. D_p is the particle diameter, and μ is the dynamic viscosity of the carrier gas.

$$v_p = \frac{D_p^2 \cdot g \cdot (\rho_p - \rho_g)}{18 \cdot \mu} \tag{7}$$

Where g is the gravitational acceleration constant. Equation (7) is only valid for $10^{-4} < Re_p < 1$. Within this limit the flow is in the Stokes regime. I.e. it is assumed that the flow is strictly laminar. This must be checked by calculating he Reynolds number. An example can be seen in section B.5. For Reynolds number in the range 2 to 400 equation (8) can be used instead. Here the Reynolds number must likewise be tested

*In Kemiske Enhedsoperationer by Clement et al.[S15] the correlations are given in equation (7.8)

to see if it is within the given range. For flow with a Reynolds number between 1 and 2 the correlation given by Oseen[S15†] can be used. They are not relevant for the data used here, so the reader is encouraged to seek more information if relevant.

$$v_p = 0.153 \cdot \left(\frac{(\rho_p - \rho_g) \cdot D_p^{1.6} \cdot g}{\mu^{0.6} \cdot \rho_g^{0.4}} \right)^{0.714} \tag{8}$$

The Prandtl Number is given in equation (9).

$$Pr = \frac{C_{p,g} \cdot \mu}{k} \tag{9}$$

B.4 Calculating the Heating Rate

The Nusselt number is approximately 2 for very small particles,[S16] but it has an increasing influence the larger the particles. To ensure consistency it is here calculated regardless of particle size. Numerous numerical correlations between Nu, Re, and Pr exist.[S17,S18‡] A simple and widely used[S19] correlation to calculate the averaged nusselt number for flow around a sphere was presented by Ranz and Marshall[S17,S20§] and is given in equation (10).

$$Nu = 2 + 0.6 \cdot Re^{1/2} \cdot Pr^{1/3} \tag{10}$$

Furthermore the Nusselt number is defined as in equation (11).

$$Nu = \frac{h \cdot D_p}{k} \Leftrightarrow h = \frac{Nu \cdot k}{Dp} \tag{11}$$

Heat transfer through thermal conduction is described in chapter 14.1 in Transport Phenomena, equation 14.1-1.[S17] Heat transfer through radiation is described in section 16.5. From these the heating rate of a solid sphere can be calculated assuming the sphere is uniform and isothermal. The equation for calculating the heating rate is given in equation (12).

$$HR = \frac{1}{C_{p,p} \cdot \rho_p \cdot \frac{4}{3} \cdot \pi (\frac{D_p}{2})^3} \cdot 4 \cdot \pi \cdot (\frac{D_p}{2})^2 \cdot ((T - T_i) \cdot h + \epsilon\sigma(T_g^4 - T^4)) \tag{12}$$

B.5 Example of Estimating the Heating Rate

Usually the given parameters in papers and for experiments are the chemical composition of carrier gas, biomass type, biomass particle diameter, final temperature of reactor system (assuming particle has same final temperature), diameter and volumetric flowrate at normal conditions for the reactor. From this the heating rate should be estimated. The example given here is based on data from DallOra et al.[S3] The necessary data are given in table S8. All numbers in the following subchapter have been rounded due to practical reasons. The calculations are made with all available decimals.

Table S8: Example of data for calculating the heating rate. From Dall'Ora et al.[S3]

Variable	Value	Unit
D_p	$0.1075 \cdot 10^{-3}$	m
T_{end}	1073	K
Biomass Type	Pine Wood	

The temperature is the first thing to calculate. It is assumed that the appropriate temperature is the average between the initial and the final temperature as given in equation (1). For the example given here it is calculated in equation (13).

$$T = 298K + \frac{1073K - 298K}{2} = 686\,K \tag{13}$$

†Information is give on page 185

‡In Transport Phenomena by Bird et al.[S17], the corelations are given in table 14.2-1

§Tn the book Transport Phenomena by Bird et al.[S17] the correlation in presented on page 439, eq. 14.4-5

Since the carrier gas is Nitrogen gas, N_2, the correlations given in equation (2) through (5) can be used to calculate the gas parameters. As these are necessary for subsequent calculations, they are calculated in equation (14) through (17) for convenience.

$$\rho_g = \frac{341.36}{686} = 0.498\, kg/m^3 \tag{14}$$

$$\mu = 3 \cdot 10^{-15} \cdot 686^3 - 2 \cdot 10^{-11} \cdot 686^2 + 0.0508 \cdot 10^{-6} \cdot 686 + 4.2787 \cdot 10^{-6} = 30.7 \cdot 10^{-6}\, Pa \cdot s \tag{15}$$

$$C_{p,g} = 19.50583 + 19.88705 \cdot 0.686 - 8.598535 \cdot 0.686^2 + 1.369784 \cdot 0.686^3 + 0.527601 \cdot (\frac{1000}{686})^2 = 30.7\, J/(kg \cdot K) \tag{16}$$

$$k = -7 \cdot 10^{-9} \cdot 686^2 + 7 \cdot 10^{-5} \cdot 686 + 0.0069 = 0.0516\, J/(s \cdot m \cdot K) \tag{17}$$

If $10^{-4} < Re < 1$ then equation (18) is valid. It is here assumed to be correct and the Reynolds number is then subsequently checked to verify.

$$v_p = \frac{(0.1075 \cdot 10^{-3} m)^2 \cdot 9.81 m/s^2 \cdot (600 kg/m^3 - 0.498 kg/m^3)}{18 \cdot 30.7 \cdot 10^{-6} Pa \cdot s} = 0.123\, m/s \tag{18}$$

Checking the Reynolds Number is done in equation (19).

$$Re = \frac{0.498 kg/m^3 \cdot 0.123 m/s \cdot 0.1075 \cdot 10^{-3} m}{30.7 \cdot 10^{-6} Pa \cdot s} = 0.215 \tag{19}$$

Since the Reynolds number check holds up, the equation chosen to calculate the velocity is appropriate. The Prandtl Number is calculated in equation (20) by using equation (9).

$$Pr = \frac{30.7 J/kg \cdot K) \cdot 30.7 \cdot 10^{-6} Pa \cdot s}{0.0516 J/(s \cdot m \cdot K)} = 0.0182 \tag{20}$$

When the Reynold Number and the Prandtl Number have been calculated the Nusselt Number can be calculated from equation(10). For this example the Nusselt Number is given in equation (21).

$$Nu = 2 + 0.6 \cdot 0.215^{1/2} \cdot 0.0182^{1/3} = 2.07 \tag{21}$$

Using equation (11) the convective heat transfer coefficient can be calculated as in equation (22).

$$h = \frac{2.07 \cdot 0.0516 J/(s \cdot m \cdot K)}{0.1075 \cdot 10^{-3} m} = 995\, J/(s \cdot m^2 \cdot K) \tag{22}$$

And finally the heating rate can be calculated from equation (12) as shown in equation (23).

$$HR = \frac{4 \cdot \pi \cdot (\frac{0.1075 \cdot 10^{-3} m}{2})^2}{1798 J/(kg \cdot K) \cdot 600 kg/m^3 \cdot \frac{4}{3}\pi (\frac{0.1075 \cdot 10^{-3}}{2})^3} \cdot \left((686K - 298K) \cdot 995 J/(s \cdot m^2 \cdot K) + 0.85 \cdot 5.670367 \cdot 10^{-8} J/(S \cdot m^2 \cdot K^4) \cdot ((1073K)^4 - (686)^4) \right) = 22703\, K/s \tag{23}$$

C Estimating the Potassium Content

The potassium content is rarely given in papers and must consequently be estimated. This estimation is here only done when the fraction of ash in the biomass used for experiments is known in order to ensure at least some accuracy. In that case the percentage of potassium in a biomass sample of the same species can be found in literature and this fraction is then assumed to be reasonably close to the real value. The reason for using the original ash fraction to estimate the potassium content is to minimize the potential error due to estimation.

C.1 Example of Estimating the Potassium Content

Dupont et al.[S21] have made high heating rate experiments, where the potassium content for the biomass is not stated. The biomass is a mixture of sylvester pine and spruce. The fraction of the two is not given, so the potassium content for sylvester pine stem wood is found in in a paper by Filbakk et al.[S22] and it is assumed to be representative. According to Filbakk et al the potassium content in sylvester pine is 76 g/kg ash. Using Dupont et al.[S21] as example the necessary parameters are given in table S9.

Table S9: Example of parameters for estimating the potassium content.

Parameter	Value	Unit	Source
Potassium Content in sylvester pine	76	g/kg ash	[S22]
Ash content in original biomass	2.1	wt% db	[S21]

The potassium content in wt% daf is calculated in equation (24).

$$c_K = \frac{76 g/kg\, ash}{1000 g\, ash/kg\, ash} \cdot \frac{2.1 g\, ash}{100 g\, biomass\,(db)} \cdot \frac{100 g\, biomass\,(db)}{(100-2.1) g\, biomass\,(daf)} = 0.163 wt\% daf \qquad (24)$$

D PCA

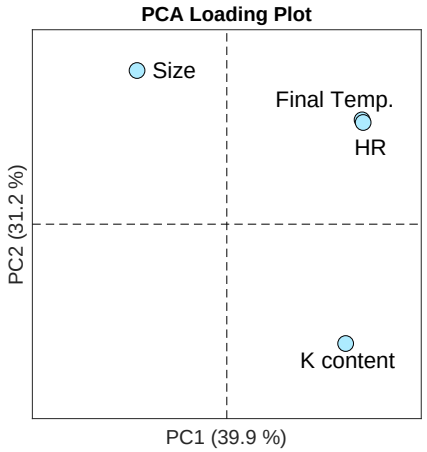

Figure S5: The loading plot for figure 1a. Final temperature and heating rate are positioned almost identically in the loading plot, because they are strongly correlated. HR = Heating rate.

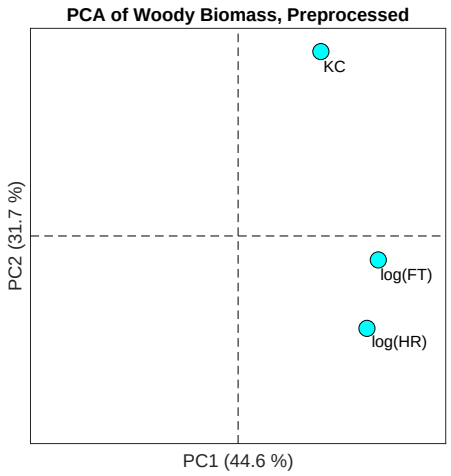

Figure S6: The loading plot for figure 1b. HR = Heating rate, FT = Finalt temperature, KC = potassium content.

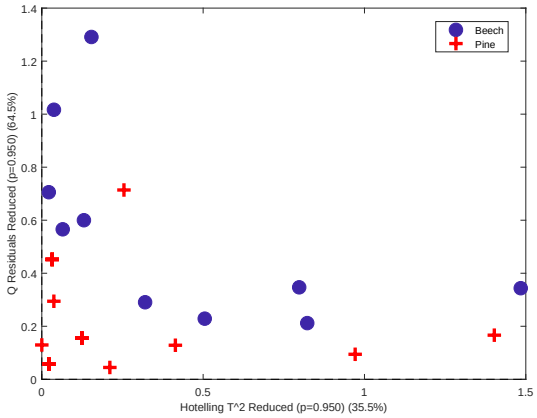

Figure S7: The Q residuals as a function of Hotelling's T^2 for model 10. No outliers are identified. Some pine data points are located identically, which is why only ten points can be seen in the plot.

References

[S1] Anna Trubetskaya, Peter Arendt Jensen, Anker Degn Jensen, Angel David Garcia Llamas, Kentaro Umeki, and Peter Glarborg. Effect of fast pyrolysis conditions on biomass solid residues at high temperatures. *Fuel Process. Technol.*, 143:118–129, 2016. ISSN 03783820. doi: 10.1016/j.fuproc.2015.11.002.

[S2] Anna Trubetskaya, Peter Arendt Jensen, Anker Degn Jensen, Markus Steibel, Hartmut Spliethoff, and Peter Glarborg. Influence of fast pyrolysis conditions on yield and structural transformation of biomass chars. *Fuel Process. Technol.*, 140:205–214, 2015. ISSN 03783820. doi: 10.1016/j.fuproc.2015.08.034.

[S3] Michelangelo Dall'Ora, Peter Arendt Jensen, and Anker Degn Jensen. Suspension Combustion of Wood: Influence of Pyrolysis Conditions on Char Yield, Morphology, and Reactivity. *Energy Fuels*, 22(5):2955–2962, 2008.

[S4] Santiago Septien, Sylvie Valin, Capucine Dupont, Marine Peyrot, and Sylvain Salvador. Effect of particle size and temperature on woody biomass fast pyrolysis at high temperature (1000 - 1400 °C). *Fuel*, 97:202–210, 2012. ISSN 0016-2361. doi: 10.1016/j.fuel.2012.01.049. URL `http://dx.doi.org/10.1016/j.fuel.2012.01.049`.

[S5] Yan Zhang, Shiro Kajitani, Masami Ashizawa, and Kouichi Miura. Peculiarities of Rapid Pyrolysis of Biomass Covering Medium- and High-Temperature Ranges. *Energy Fuels*, 20(6):2705–2712, 2006.

[S6] L. Chen, C. Dupont, S. Salvador, M. Grateau, G. Boissonnet, and D. Schweich. Experimental study on fast pyrolysis of free-falling millimetric biomass particles between 800 °c and 1000 °c. *Fuel*, 106:61 – 66, 2013. ISSN 0016-2361.

[S7] Santiago Jiménez, Pilar Remacha, Juan C Ballesteros, Antonio Giménez, and Javier Ballester. Kinetics of devolatilization and oxidation of a pulverized biomass in an entrained flow reactor under realistic combustion conditions. *Combust. Flame*, 152(4):588–603, 2008. doi: 10.1016/j.combustflame.2007.10.001.

[S8] M.G. Grønli. *A theoretical and experimental study of the thermal degredation of biomass.* PhD thesis, NTNU, 1996.

[S9] Yoshio Kijidani and Yoshimitsu Fujii. Microfibril angle and density of hinoki (Chamaecyparis obtusa) trees in 15 half-sib families in a progeny test stand in Kyushu, Japan. *Journal of Wood Science*, 58 (3):195–202, 2012. doi: 10.1007/s10086-011-1240-8.

[S10] EngineeringToolbox. Densities of wood species. `http://www.engineeringtoolbox.com/wood-density-d\_40.html`, 2016. Accessed: 2018-02-23, Last Modified: 2016-06-03.

[S11] P. J. Linstrom and W. G. Mallard, editors. *"Fundamental Physical Constants, Stefan Boltzmann constant" in NIST Chemistry WebBook, NIST Standard Reference Database Number 69.* National Institute of Standards and Technology, Gaithersburg MD, 20899, 2014. URL `https://physics.nist.gov/cgi-bin/cuu/Value?sigma`.

[S12] Morten G. GrÃ¸nli and Morten C. Melaaen. Mathematical model for wood pyrolysiscomparison of experimental measurements with model predictions. *Energy & Fuels*, 14(4):791–800, 2000. doi: 10.1021/ef990176q.

[S13] M.O. McLinden E.W. Lemmon and D.G. Friend. *"Thermophysical Properties of Fluid Systems" in NIST Chemistry WebBook, NIST Standard Reference Database Number 69.* National Institute of Standards and Technology, Gaithersburg MD, 20899, 2005. URL `http://webbook.nist.gov`.

[S14] Osborne Reynolds. Xxix. an experimental investigation of the circumstances which determine whether the motion of water shall he direct or sinuous, and of the law of resistance in parallel channels. *Philosophical Transactions of the Royal Society of London*, 174:935–982, 1884. doi: 10.1098/rstl.1883.0029. URL `http://rstl.royalsocietypublishing.org/content/174/935.short`.

[S15] K.H. Clement, P. Fangel, A.D. Jensen, and K. Thomsen. *Kemiske Enhedsoperationer*, volume 5. Polyteknisk Forlag, 2 edition, 2009. ISBN 8750209418.

[S16] Zhipeng Duan, Boshu He, and Yuanyuan Duan. Sphere Drag and Heat Transfer. *Nature Publishing Group*, pages 1–7, 2015. doi: 10.1038/srep12304. URL `http://dx.doi.org/10.1038/srep12304`.

[S17] R.B. Bird, W.E. Stewart, and E.N. Lightfoot. *Transport Phenomena*, volume 1. John Wiley & sons, Inc., rev. 2nd edition, 2007. ISBN 9780470115398.

[S18] Andreas Richter and Petr A Nikrityuk. International Journal of Heat and Mass Transfer Drag forces and heat transfer coefficients for spherical , cuboidal and ellipsoidal particles in cross flow at sub-critical Reynolds numbers. *International Journal of Heat and Mass Transfer*, 55(4):1343–1354, 2012. ISSN 0017-9310. doi: 10.1016/j.ijheatmasstransfer.2011.09.005. URL `http://dx.doi.org/10.1016/j.ijheatmasstransfer.2011.09.005`.

[S19] Kentaro Umeki, Kawnish Kirtania, Luguang Chen, and Sankar Bhattacharya. Fuel Particle Conversion of Pulverized Biomass during Pyrolysis in an Entrained Flow Reactor. *Ind. Eng. Chem. Res.*, 51(43): 13973–13979, 2012.

[S20] W.E. Ranz and W.R. Marshall. Evaporation from Drops: Part 2. *Chemical Engineering Progress*, 48 (4):173–180, 1952.

[S21] Capucine Dupont, Jean-Michel Commandré, Paola Gauthier, Guillaume Boissonnet, Sylvain Salvador, and Daniel Schweich. Biomass pyrolysis experiments in an analytical entrained flow reactor between 1073 K and 1273 K. *Fuel*, 87(7):1155–1164, 2008. doi: 10.1016/j.fuel.2007.06.028.

[S22] Tore Filbakk, Raida Jirjis, Juha Nurmi, and Olav Høibø. The effect of bark content on quality parameters of Scots pine (Pinus sylvestris L .) pellets. *Biomass and Bioenergy*, 35(8):3342–3349, 2010. ISSN 0961-9534. doi: 10.1016/j.biombioe.2010.09.011. URL `http://dx.doi.org/10.1016/j.biombioe.2010.09.011`.